Biol Cybern (2008) 98:133–143
DOI 10.1007/s00422-007-0197-6

ORIGINAL PAPER

Biological Cybernetics

Nonlinearities make a difference: comparison of two common Hill-type models with real muscle

Tobias Siebert · Christian Rode · Walter Herzog · Olaf Till · Reinhard Blickhan

Received: 9 August 2007 / Accepted: 25 October 2007 / Published online: 30 November 2007

Abstract Compared to complex structural Huxley-type models, Hill-type models phenomenologically describe muscle contraction using only few state variables. The Hill-type models dominate in the ever expanding field of musculoskeletal simulations for simplicity and low computational cost. Reasonable parameters are required to gain insight into mechanics of movement. The two most common Hill-type muscle models used contain three components. The series elastic component is connected in series to the contractile component. A parallel elastic component is either connected in parallel to both the contractile and the series elastic component (model [CC+SEC]), or is connected in parallel only with the contractile component (model [CC]). As soon as at least one of the components exhibits substantial nonlinearities, as, e.g., the contractile component by the ability to turn on and off, the two models are mechanically different. We tested which model ([CC+SEC] or [CC]) represents the cat soleus better. Ramp experiments consisting of an isometric and an isokinetic part were performed with an in situ cat soleus preparation using supramaximal nerve stimulation. Hill-type models containing force–length and force–velocity relationship, excitation–contraction coupling and series and parallel elastic force–elongation relations were fitted to the data. To test which model might represent the muscle better, the obtained parameters were compared with experimentally determined parameters. Determined in situations with negligible passive force, the force–velocity relation and the series elastic component relation are independent of the chosen model. In contrast to model [CC+SEC], these relations predicted by model [CC] were in accordance with experimental relations. In conclusion model [CC] seemed to better represent the cat soleus contraction dynamics and should be preferred in the nonlinear regression of muscle parameters and in musculoskeletal modeling.

T. Siebert (✉) · C. Rode · O. Till · R. Blickhan
Institute of Motion Science, Friedrich Schiller University,
Seidelstraße 20, 07749 Jena, Germany
e-mail: tobias.siebert@uni-jena.de

W. Herzog
Faculty of Kinesiology, University of Calgary,
2500 University Drive, NW, Calgary, AB T2N1N4, Canada

1 Introduction

Mathematical models of skeletal muscle play an important role in the simulation of movement (van Soest and Bobbert 1993; van Soest et al. 2003; Wagner and Blickhan 2003) and the understanding of control mechanisms (Blickhan et al. 2003). Although many phenomenological and biophysiological models have been developed to represent the dynamics of isolated muscles (Winters and Woo 1990), the phenomenological modelling approach based on Hill (1938) dominates in modeling of muscle skeletal systems for simplicity and low computational cost.

Hill-type model parameters have been determined in many different ways, for example by performing special experiments on isolated muscles (e.g., Curtin et al. 1998). However, these methods are time consuming and limited when determining model parameters for in vivo human muscles. Therefore, a second strategy has emerged in which human muscle model parameters were determined using nonlinear regression to approximate selected experimental data (Wagner et al. 2006; Siebert et al. 2007). However, one difficulty with this approach is the lacking representation of passive forces.

In real muscle, the contractile elements are surrounded by passive tissues that can be represented as elastic in a first order approximation. These passive structures are usually divided into components thought to act purely in series (SEC)

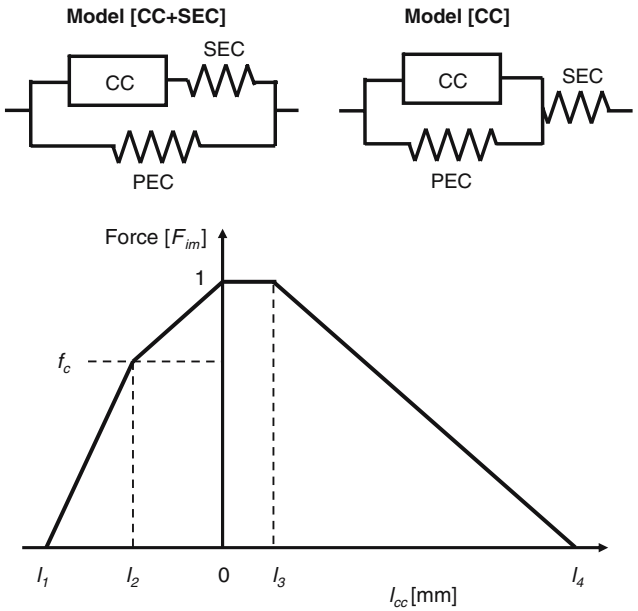

Fig. 1 Principal connection schemes (*top*) of contractile component (*CC*), series elastic component (*SEC*) and parallel elastic component (*PEC*), where (*top*, *left*) is referred to as model [CC+SEC] and (*top*, *right*) is referred to as model [CC] throughout the manuscript. The force–length relationship (*bottom*) was normalized relative to F_{im} and described with a piecewise linear model. l_2 was the length, at which the ascending limb changed slope, and f_c the corresponding force. l_3 equalled the length of the plateau, and l_1 and l_4 determined the width of the force–length relationship

and purely in parallel (PEC) to the contractile component (CC) in classical Hill-type models. Two principal Hill-type models have emerged: one in which the passive component (PEC) is arranged in parallel with the CC and the SEC (model [CC+SEC]) (Fig. 1, top left); the other, in which the PEC is only in parallel with CC (model [CC]) (Fig. 1, top right). Both models have been used in the past to represent muscle contraction (e.g., Ettema and Meijer 2000; van Soest et al. 2003). However, in the range in which passive properties are not negligible, muscle parameters describing the contractile properties, such as the active force–length relationship and the force–elongation relation of the parallel elastic element, are highly dependent on the model of choice ([CC+SEC] or [CC]) (Rode et al. 2007).

The purpose of this study was to determine phenomenological muscle parameters by nonlinear regression for situations with pronounced parallel elasticity and to test which model ([CC+SEC] or [CC]) might represent the cat soleus better. To achieve this goal, carefully selected experiments were performed. Data were approximated in a single regression analysis by adapting all parameters of model [CC+SEC] and [CC], respectively. These parameters were compared with parameters resulting from experiments and literature.

2 Methods

2.1 Experimental setup

Experiments were performed on four cat soleus muscles (index SOL1–SOL4). The experimental setup and protocol used in this study were approved by the Life Sciences Animal Ethics Committee of the University of Calgary. The detailed approach and methods can be found in Herzog and Leonard (1997).

Briefly, adult outbred cats weighing from 2.8 to 3.3 kg were anesthetized using a 5% halothane gas mixture; then they were intubated and maintained at 1% halothane. The soleus muscle and tendon were exposed with a single cut on the posterior lateral shank. Then, the muscle was isolated by severing the tendons of the remaining ankle extensors, and by cutting the soleus tendon from the calcaneus including a bone fragment. A second cut was made on the posterior, lateral thigh and the tibial nerve was exposed and instrumented with a bipolar cuff-type electrode for soleus stimulation (Herzog et al. 1995). The cat was secured in a prone position in a hammock and the pelvis, thigh, and shank of the experimental hindlimb were fixed with bilateral bone pins to a stereotaxic frame. In addition, a heating pad was placed below the animal and the soleus temperature was kept between 35 and 36.5°C. Finally, the bone fragment at the distal end of the soleus tendon was attached to a muscle puller (MTS, Eden Prairie, MN), which recorded the muscle's length change (5 mm/V) and force (10 N/V) with a sampling frequency of 250 Hz for isometric and 1,000 Hz for dynamic conditions.

To activate the soleus muscle, the tibial nerve was stimulated supramaximally using a current pulse with amplitude of three times the alpha motoneuron threshold, a pulse duration of 100 μs, and a frequency of 30 Hz. This stimulation method ensured fused tetanic contraction of the cat soleus (Herzog and Leonard 1997).

2.2 Experimental protocol

Muscle lengths at which passive force reached 1 N was defined as a reference length, and is hereafter designated as the 0 mm length. This length is slightly below the optimal length (Herzog and Leonard 2000). The muscle was then shortened by 12 mm (−12 mm) to a position, at which the tendon was visibly slack (resting position). Rest between the contractions was 60 s, which was sufficient to avoid fatigue (Herzog and Leonard 1997). All experiments followed the same protocol. The muscle was pulled passively from −12 mm to the starting length, and after 3 s, when the passive force transients had almost disappeared, the experiments started. Four seconds after the end of a test contraction, the muscle was moved back to the resting position.

Isometric reference contractions at a muscle length of +12 mm were performed throughout the experiments, and force loss due to fatigue (which never exceeded 5%) was accounted for by adjusting reference forces to 100% at all times.

2.2.1 *Ramp experiments used for nonlinear regression of model parameters*

Ramp experiments consisting of an initial isometric part and subsequent isokinetic shortening from +12 to −24 mm and speeds of 5, 10, 20, 40, 70, 100, and 150 mm/s (Fig. 2d) were performed. Isokinetic shortening began 1 s after the onset of stimulation, which was continued throughout the ramp experiments. All experiments were repeated passively.

Passive force of SOL2 exceeded 0.6 of the total force at +12 mm. To avoid muscle damage, passive and active isokinetic ramps were performed from +10 to −26 mm for this muscle.

2.2.2 *Experimental force–velocity and force–length relationships*

The force–velocity relationship was determined in situations with negligible passive force with six to eight step-and-ramp shortening experiments as performed by Curtin et al. (1998). The step distance was adjusted for each shortening velocity such that force transients in the isokinetic ramp part were minimized. Depending on step distance, experiments started at muscle lengths ranging from +7 to +9 mm, reaching constant forces at lengths ranging from 0 to +2 mm. Force values obtained during isokinetic shortening were normalized relative to the isometric forces at the corresponding lengths.

For the active force–length relationship, total and passive isometric forces were measured at 2 mm length increments from −24 to +12 mm, where the total and the passive forces are the forces exerted by the muscle in presence and in absence of stimulation at the same length, respectively. Soleus was stimulated for 3 s and the maximum total isometric force was determined. Assuming model [CC+SEC], one obtained active forces by subtracting passive from total force. Assuming model [CC], the active force–length relationship was determined using the method proposed by Rode et al. (2007). The required PEC and SEC force–elongation relations were taken from the nonlinear regression results (Table 2).

Parameters characterizing the relationships obtained from these experiments are termed experimental parameters (please see Table 1).

2.3 Models

The force generated by the CC is a function of the activation state $A \in [0, 1]$, the maximum active isometric force (F_{im}),

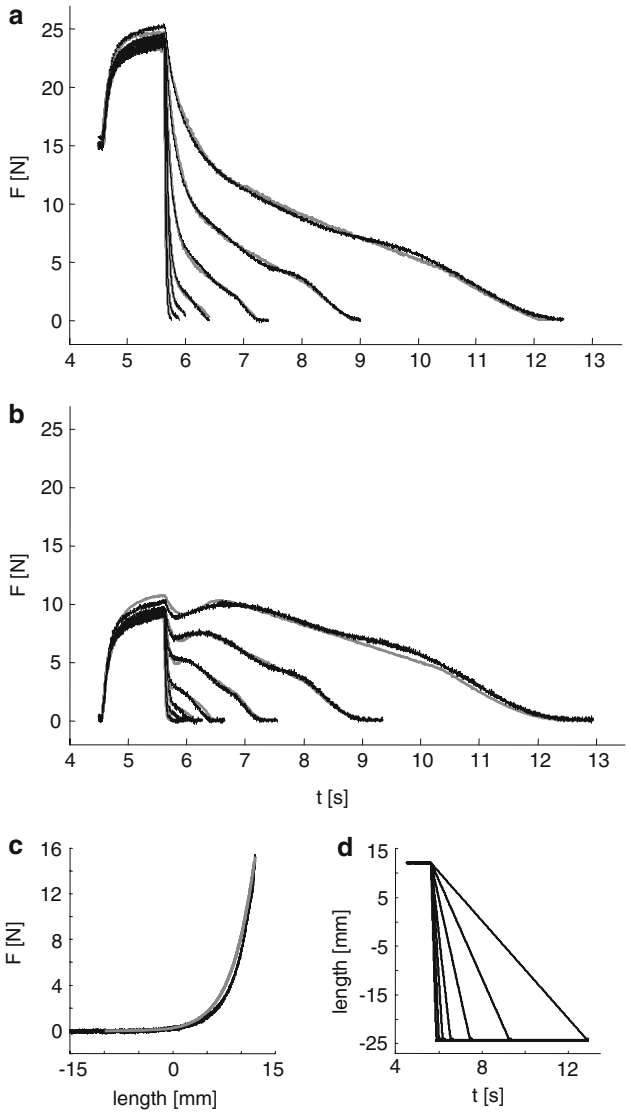

Fig. 2 Exemplar (SOL2) measured data (*black lines*) used for the regression of model parameters, and simulated forces (*grey lines*) using the parameters from Table 2. **a**, **c** The measured total **a** and passive forces **c** from ramp experiments (*black lines*) as well as total **a** and passive force **c** simulated using model [CC] (*grey lines*). **b** Forces calculated by subtracting the measured passive **c** from the total forces **a** (*black lines*), which correspond to the force in the CC using model [CC+SEC], and the simulated CC force using model [CC+SEC] (*grey lines*). **d** Ramp experiments had an isometric part followed by isokinetic shortening at different velocities (5, 10, 20, 40, 70, 100 and 150 mm/s)

the force–length (f_l), and the force–velocity (f_v) relationships:

$$F_{\mathrm{CC}}(A, f_l, f_v, F_{\mathrm{im}}) = A(S) \cdot f_l(l_{\mathrm{CC}}) \cdot f_v(v_{\mathrm{CC}}) \cdot F_{\mathrm{im}}. \quad (1)$$

Rode et al. (2007) have shown that the active soleus force–length relationship approximates the theoretical sarcomere force–length relationship (Herzog et al. 1992) within the tested length range. Therefore, the CC force–length relationship was described with a piecewise linear equation:

Table 1 Nomenclature of the methods used for muscle parameter determination

Model	Name of parameters	Method of determination			
		Force–length	Force–velocity	SEC	PEC
Model [CC+SEC]	Fitted	Adaptation of all model parameters to data from ramp experiments			
Model [CC]		Adaptation of all model parameters to data from ramp experiments			
Model [CC+SEC]	Experimental	Subtraction of passive from total isometric force			From passive measure
Model [CC]		Subtraction of reduced passive force from total isometric force (Rode et al. 2007)			
Model [CC+SEC]	Experimental		Step-and-ramp shortening (Curtin et al. 1998)		
+[CC][a]	Literature			Sonometric measure	

[a] Determined in situations with negligible passive force, the force–velocity relationship (Hill 1938) and the SEC force–elongation relationship are independent of the model representation

$$f_l(l_{CC}) = \begin{cases} \frac{f_c}{l_2 - l_1} \cdot (l_{CC} - l_1), & l_1 \le l_{CC} \le l_2 \\ \frac{1 - f_p}{-l_2} \cdot (l_{CC} - l_2), & l_2 < l_{CC} \le 0 \\ 1, & 0 < l_{CC} \le l_3 \\ \frac{-1}{l_4 - l_3} \cdot (l_{CC} - l_3), & l_3 < l_{CC} \le l_4 \end{cases}, \quad (2)$$

where f_c is the force, at which the ascending limb changes slope, l_{CC} is the CC length minus the optimal CC length and l_1, l_2, l_3 and l_4 are specific lengths that are crucial for the sarcomere force–length relationship (Fig. 1 bottom).

The force–velocity relationship followed the Hill hyperbola (Hill 1938) for concentric contractions:

$$f_v(v_{CC}) = \frac{v_{CCmax} - v_{CC}}{v_{CCmax} + v_{CC} \cdot curv} \quad v_{CC} < 0, \quad (3)$$

where $v_{CCmax} < 0$ is the maximal CC shortening velocity, and curv is a curvature parameter.

The latency between a present stimulus (S) and the activation state was modelled as a first order linear differential equation (Otten 1987):

$$\frac{dA}{dt} = \frac{1}{\tau} \cdot (S - A) \quad S, A \in [0, 1], \quad (4)$$

where τ lumps the time constants of calcium influx from the sarcoplasmic reticulum into the sarcoplasm.

The SEC force–elongation relationship $F_{SEC}(\Delta l_{SEC})$ was taken from Winters and Woo (1990):

$$\begin{aligned} F_{SEC}(\Delta l_{SEC}) &= \frac{F_1}{e^{k_{sh}} - 1} \cdot \left(e^{\frac{k_{sh} \cdot \Delta l_{SEC}}{\Delta l_{SEC1}}} - 1 \right), \quad 0 < \Delta l_{SEC} < \Delta l_{SEC1} \\ F_{SEC}(\Delta l_{SEC}) &= F_1 + k \cdot (\Delta l_{SEC} - \Delta l_{SEC1}), \quad \Delta l_{SEC1} \le \Delta l_{SEC}. \end{aligned} \quad (5)$$

Δl_{SEC1} and F_1 are the length and the force at which the force–elongation relation changes from exponential to linear. k was calculated from Δl_{SEC1}, F_1, the dimensionless shape parameter k_{sh} and the constraint that stiffness at $\Delta l_{SEC} = \Delta l_{SEC1}$ was the same.

In both muscle models [CC+SEC] and [CC], the kinematic dependence of SEC and CC is

$$l_{mtc} = \Delta l_{SEC} + l_{CC} + l_m. \quad (6)$$

l_{mtc} is the length of the muscle-tendon complex, and l_m is the constant sum of the slack length of the SEC and the optimal length of the CC.

In model [CC+SEC], the force in the SEC equals the force in the CC. Using this information, the force in the CC is uniquely determined for a given muscle length and activation state, and can be obtained by integration of the following:

$$v_{CC} = \frac{dl_{CC}}{dt} = f_v^{-1}\left(\frac{F_{SEC}}{A \cdot f_l \cdot F_{im}} \right). \quad (7)$$

In model [CC], the PEC influences the intrinsic contraction dynamics. A PEC force–elongation relation $F_{PEC}(\Delta l_{PEC})$ depending on k_1 and k_2 was taken from Brown et al. (1996)

$$F_{PEC}(\Delta l_{PEC}) = k_1 \cdot \left(e^{k_2 \cdot \Delta l_{PEC}} - 1 \right), \quad \text{if } \Delta l_{PEC} > 0, \quad (8)$$

and an additional kinematic dependence arose:

$$l_{mtc} = \Delta l_{SEC} + \Delta l_{PEC} + l_{mslack}, \quad (9)$$

where l_{mslack} is the constant sum of SEC and PEC slack lengths. The force in the SEC equals the sum of the forces in the CC and the PEC. Using this information, the force in the CC is uniquely determined for a given muscle length and activation state, and can be obtained by integrating the following:

$$v_{CC} = \frac{d\Delta l_{CC}}{dt} = f_v^{-1}\left(\frac{F_{SEC} - F_{PEC}}{A \cdot f_l \cdot F_{im}}\right). \quad (10)$$

The model parameters were optimized in a single regression analysis by minimizing the square deviation (*ss*) between measured ramp experiment forces and simulated forces with a Levenberg–Marquardt algorithm. The deviations were weighted according to the number of data points of the corresponding ramp experiment. Multiple fits can help to find the optimal parameter set (Ahearn et al. 2005). The best of 50 fits using bounded random initial parameter sets yielded the resulting parameters. Model input was time dependent muscle length and stimulation for active ramps.

Using model [CC+SEC], one subtracted the forces measured in a passive ramp experiment (velocity independent, see Fig. 7b) from the total forces measured in seven active ramp experiments (5, 10, 20, 40, 70, 100, and 150 mm/s) to obtain the forces in the CC (Fig. 2b). These seven force–time data sets were then used in a single regression analysis to obtain the CC and SEC parameters. PEC parameters (Eq. 8) were separately fitted to the passive muscle force–length relation setting l_{mslack} to −10 mm (Fig. 2c).

Seven active ramp experiments (5, 10, 20, 40, 70, 100, and 150 mm/s) and one passive ramp experiment (5 mm/s) were used in a single regression analysis for all model [CC] parameters. To narrow down the space of possible solutions, the number of free parameters was reduced using present constraints. The initial passive force exerted by the muscle prior to stimulation was used to calculate k_1 in each step of the regression, and l_{mslack} was set to −10 mm, according to the data (Fig. 2c). For the passive ramp, CC forces were taken to be zero.

The length range in the ramp experiments was not sufficient to determine realistic l_4 parameters by regression for model [CC]. However, l_4 and τ influence the force rise in the isometric part of the ramp experiments. Therefore τ was determined using l_4 values calculated from the theoretical sarcomere force–length relationship (Herzog et al. 1992).

The forces at the end of the isometric part decreased in a well defined manner from the first to the last ramp experiment. This effect was accounted for by a specific F_{im} parameter for each ramp.

Means and standard deviations of all parameters were determined from both muscle models. Parameters obtained by nonlinear regression are termed fitted parameters (please see Table 1).

3 Results

The total force of all muscles decreased during the shortening phase of the ramp experiments (Fig. 2a). Passive forces during the shortening phase were nearly independent of velocity (Figs. 2c, 7b, black lines). The simulated forces approximated the data well using model [CC] and model [CC+SEC] (Fig. 2a–c, SOL2; Table 2), although the approximations were achieved with substantial differences in the model parameters.

3.1 Force–length relationship

Using the same model, experimental and fitted (compare Table 1) active force–length relationships yielded qualitatively the same shape (Fig. 3). Model [CC] always predicted an ascending limb and a plateau for the cat soleus (Fig. 3e–h, grey lines). Model [CC+SEC], predicted an active force–length relationships with a descending limb (Fig. 3a–c, grey lines) except for one muscle (SOL4; Fig. 3d, grey line).

The fitted active force–length relationships using model [CC] (Fig. 3e–h, grey lines) approximated the experimental relationships (Fig. 3e–h, filled circles) better than those using model [CC+SEC] (Fig. 3a–d). Differences in between experimental and fitted maximum active isometric force (F_{im}) were 3.5% ± 3.5 and 9.2% ± 3.0 for models [CC] and [CC+SEC], respectively (Table 3). Deviations in optimal muscle lengths were −1.2 mm ± 0.8 and 4.1 mm ± 1.4, respectively (Table 3). Model [CC] underestimated the isometric forces by up to $0.2F_{im}$ and model [CC+SEC] by up to $0.35F_{im}$ on the ascending part of the force–length relationship (Fig. 4).

Experimental and fitted F_{im} obtained using model [CC] were about 10% higher than those obtained using model [CC+SEC] (Table 3).

3.2 Force–velocity relation

All experimental force–velocity relationships had the typical hyperbolic shape observed by Hill (1938) (Fig. 5, black circles). Fitted model [CC] parameters approximated these relationships well (Fig. 5e–h). Differences in maximum power (p_{max}) were 3.6% ± 6.0 (Table 3). Fitted parameters using model [CC+SEC] overestimated the experimental data (Fig. 5a–d), which resulted in differences in maximum power of 29.9% ± 9.0 (Table 3). Model [CC+SEC] underestimated the curvature of the force–velocity relationship, resulting in small curve values (Table 2).

3.3 Force–elongation relation of SEC

The linear part of the fitted SEC force–elongation relation started at approximately $0.2F_{im}$ for model [CC+SEC] and $0.3F_{im}$ for model [CC] (Fig. 6). The stiffness in the linear part was 4 N/mm ± 1.5 for model [CC+SEC] and 8 N/mm ± 1.6 for model [CC] (Table 2).

Table 2 Single muscle parameter sets of model [CC+SEC] and [CC] based on the corresponding ramp experiments

	Model [CC+SEC]				Model [CC]			
	SOL1	SOL2	SOL3	SOL4	SOL1	SOL2	SOL3	SOL4
l_1[mm]	−23	−23	−22	−24	−24	−22	−21	−27
l_2[mm]	−14	−18	−14	−11	−14	−15	−14	−13
l_3[mm]	2	0	2	4	4	6	1	1
l_4[mm]	19	17	13	14	8 (36)	8 (33)	67 (31)	6 (40)
$f_c[F_{\text{im}}]$	0.49	0.41	0.43	0.71	0.51	0.42	0.41	0.69
$v_{\max}$[mm/s]	−141	−138	−124	−160	−152	−184	−176	−141
curv	5.8	6.4	8.8	10.4	9.5	16.9	19.5	13.6
k_1[N]	0.0120	0.0062	0.0011	0.028	0.0064	0.0021	0.0012	0.0461
k_2[mm^{-1}]	0.317	0.351	0.442	0.278	0.414	0.490	0.525	0.300
F_1[N]	4.1	3.2	3.3	8.6	8.9	10.2	4.6	5.9
d_{LSEC1}[mm]	4.1	5.6	3.7	2.7	2.9	3.3	2.6	2.2
ksh	3.3	4.3	3.0	1.4	2.5	2.6	3.7	3.9
k [N/mm]	3.5	2.5	2.8	5.9	8.2	8.5	6.6	10.5
l_m[mm]	0.3	0.1	0.3	3.2	2.6	1.5	1.1	6.2
F_{im}[N]	18.1	13.7	13.2	21.8	20.6	15.9	15.2	26.7
τ [s]	0.006	0.008	0.004	0.024	0.065	0.070	0.080	0.080
ss[N^2]	2,873	1,828	947	1,891	1,585	1,398	1,189	3,183

τ values for model [CC] result from simulations with l_4 parameters in brackets according to the theoretical sarcomere force–length relationship (Herzog et al. 1992). *ss* is the minimal square deviation between measured force and simulated force of all active ramp experiments at the end of the regression process

Table 3 Selected representative muscle parameters obtained experimental (exp.) and by nonlinear regression (fitted) based on model [CC+SEC] and model [CC]

		SOL1	SOL2	SOL3	SOL4
Model [CC+SEC]	F_{im} exp. [N]	20.0	15.7	14.2	23.5
	F_{im} fitted [N]	18.1	13.7	13.2	21.8
	difference [%]	9.4	13.3	6.7	7.3
	l_{mopt} exp. [mm]	4	4	4	6
	l_{mopt} fitted [mm]	8.4	9.8	7.6	8.6
	difference [mm]	−4.4	−5.8	−3.6	−2.6
	$p_{\max}$ exp. [$F_{\text{im}}\times$ mm/s]	8	7.1	6.1	6.7
	$p_{\max}$ fitted [$F_{\text{im}}\times$ mm/s]	10.8	9.9	7.3	8.4
	difference [%]	−35.0	−39.4	−19.7	−25.4
Model [CC]	F_{im} exp. [N]	21.6	17.2	15.1	27.5
	F_{im} fitted [N]	20.6	15.9	15.2	26.7
	difference [%]	4.6	7.4	−1.0	3.0
	l_{mopt} exp. [mm]	8	8	6	12
	l_{mopt} fitted [mm]	7.2	5.6	5.4	11
	difference [mm]	0.8	2.4	0.6	1
	$p_{\max}$ exp. [$F_{\text{im}}\times$ mm/s]	8	7.1	6.1	6.7
	$p_{\max}$ fitted [$F_{\text{im}}\times$ mm/s]	8.4	6.7	5.8	6.1
	difference [%]	−5.0	5.6	4.9	9.0

The length at which the increase in active force was smaller than 1% F_{im} was determined as the beginning of the plateau of force–length relationship (l_{mopt})

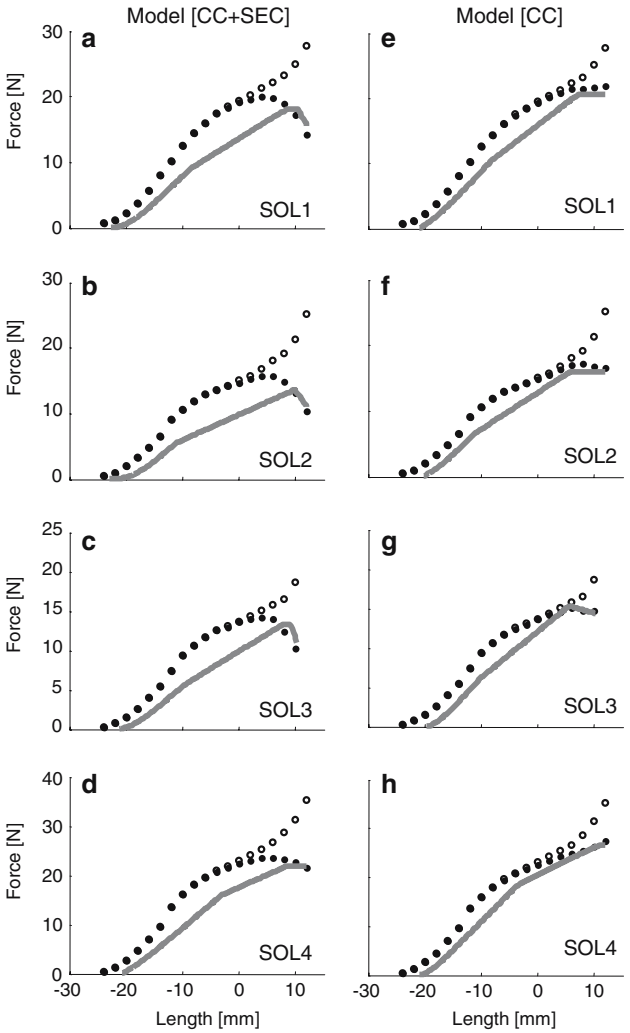

Fig. 3 Active force–length relationships applying model [CC+SEC] **a–d** and model [CC] **e–h**. Fitted active force–length relationships (*grey lines*), using ramp experiment data, underestimate experimental (see Sect. 2) active force–length relationships (*filled circles*). The very low slope of the descending limb of the fitted SOL3 (model [CC]) force–length relationship was interpreted as plateau. For better orientation all pictures contain the measured isometric total force–length relationships (*unfilled circles*). Note that muscle length [mm] includes SEC elongation

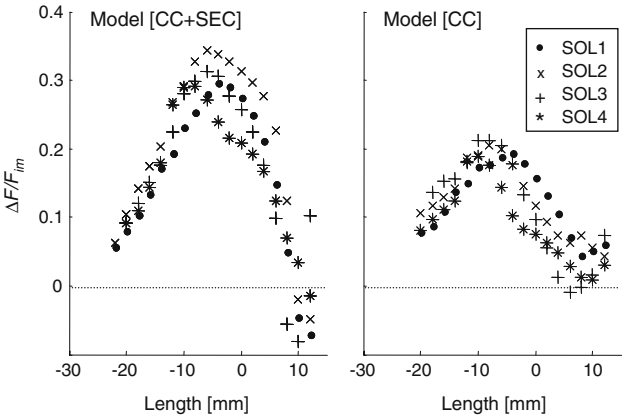

Fig. 4 Force differences (ΔF) between experimental and fitted active force–length relationships (Fig. 3, *grey lines* and *filled circles*, respectively) normalized to the corresponding experimental F_{im}. The deviation is higher in model [CC+SEC] especially in the plateau region of the active force–length relationship

3.4 Force–elongation relation of PEC

All muscles showed similar passive force–length behaviour (Fig. 7a, black lines). Model [CC] predicted consistently stiffer PEC force–elongation relations (Fig. 7a, grey lines) than model [CC+SEC].

4 Discussion

The aims of the present study were to determine consistent phenomenological model [CC+SEC] and model [CC] parameter sets by nonlinear regression to various dynamic contractions and to test which model might represent the cat soleus better. While Rode et al. (2007) focussed on differences in the model [CC+SEC] and model [CC] active force–length relationships (calculated from isometric experiments) and the impact on the interpretation of muscle experiments, this study uses a novel method to choose the more appropriate model.

As long as a muscle works within a range in which passive forces are negligible, the two model representations are equivalent, and contractile properties, such as the force–velocity relationship (Hill 1938) and SEC force–elongation properties, can be obtained readily. Deviating PEC force–elongation relation and active force–length relationship result from the structural difference of the models. Therefore, by comparing the fitted SEC force–elongation relation and the fitted force–velocity relation with experimental data, a decision may be made which model represents the cat soleus phenomenologically better.

For model [CC], the fitted force–velocity relationship agrees with the experimental soleus force–velocity relationship and literature data (Scott et al. 1996). Also, the fitted SEC stiffness for forces higher than $0.2F_{\mathrm{im}}$ ($k = 8\,\mathrm{N/mm} \pm 1.6$, Table 2) is comparable to soleus muscle stiffness (11 N/mm) from Proske and Morgan (1984). In contrast, using model [CC+SEC] in the regression lead to an unrealistic compliant SEC ($4\,\mathrm{N/mm} \pm 1.5$) and deviating force–velocity relationship (Fig. 5). Nonlinear regression based on model [CC+SEC] yielded SEC strains at F_{im} in the range of 10% (Fig. 6, model [CC+SEC]), which were in the strain region of 10–15% where tendon rupture can be expected (Fung 1993). Therefore, we conclude that model [CC] better captures the contraction dynamics of cat soleus than model [CC+SEC] and should be preferred in the nonlinear regression of muscle parameters.

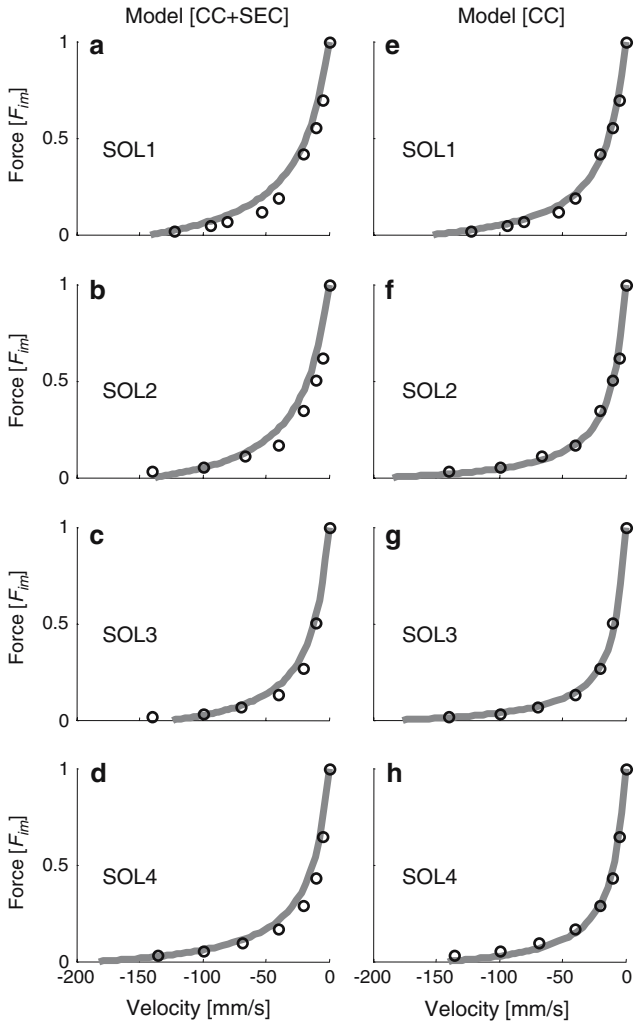

Fig. 5 Fitted force–velocity relations (*grey lines*) of model [CC+SEC] **a–d** and model [CC] **e–h** compared to experimental force–velocity relations (*black circles*). Force–velocity relations obtained by regression of model [CC+SEC] underestimate the curvature (Table 2) and overestimate normalized maximum power output (Table 3)

The application of model [CC+SEC] in the regression and later in simulations might lead to erroneous results. Suppose a given isometric force at a length with negligible passive force and linear SEC compliance. The parameters presented suggest a nearly twice as long SEC elongation for model [CC+SEC] compared to model [CC]. The energy stored in model [CC+SEC] SEC would be twice the energy as in the model [CC] SEC, since the energy in a linear spring depends quadratic on elongation. Also, metabolic costs of such contractions would be overestimated applying a velocity dependent metabolic cost function (van Leeuwen 1992).

4.1 Prediction of ramp experiments

Rather surprisingly, despite the differences in the parameters both models were able to approximate the experimental data with similar square deviations *ss* (Model [CC+SEC]: $ss = 1885 \pm 787\,\mathrm{N}^2$; Model [CC]: $ss = 1839 \pm 910\,\mathrm{N}^2$, Table 2).

A more compliant SEC leads to a slower force rise after the onset of stimulation in an isometric muscle contraction due to higher contraction velocity of the contractile elements and lower f_v values. In model [CC+SEC], this effect was compensated by very small activation time constants τ (Table 2). During the isokinetic part of the ramp experiment, the unrealistically compliant SEC (Model [CC+SEC]) led to a considerable reduction of shortening velocity of the CC. Combined with lower curvature values of the force–velocity relation of model [CC+SEC] compared to model [CC] (Table 2), this resulted in high f_v values during isokinetic shortening. These f_v values compensated the highly underestimated f_l values (Fig. 3) and allowed model [CC+SEC] to reproduce the ramp experiment forces. In conclusion, the quality of the fit to experimental data alone is not necessarily a valuable criterion to decide which model is more appropriate to represent the muscle.

4.2 Physiological meaning

Recently, in a simulation study Epstein et al. (2006) demonstrated that the aponeurosis might not be arranged purely in series to the contractile component. However, the fitted SEC force–elongation relation agrees with estimated tendon and aponeurosis force–elongation relation given by Brown et al. (1996) (Fig. 6, model [CC]). Therefore, it may be concluded that aponeurosis and tendon compliance dominate SEC compliance in the cat soleus and the effect described by Epstein et al. (2006) may be less important for the cat soleus, a muscle with low fiber and aponeurosis angle (Rack and Westbury 1969).

The active force–length relation depends on the model of choice (Rode et al. 2007). Given a passive force at a constant length, higher active forces are required to produce equal total forces for model [CC] compared to model [CC+SEC]. The difference between these active forces depends on model [CC] SEC and PEC force–elongation relations. Assuming that the SEC parameters are realistic as argued above, and assuming an in series arrangement of SEC and PEC as in model [CC], fitted PEC parameters must also be reasonable, since the measured passive force–length relation of the muscle is reproduced by model [CC] (Fig. 7b). This leads to the conclusion that the experimental active force–length relationship determined from isometric measurements using model [CC] is realistic, too. However, although three fitted relationships (force–velocity relationship, SEC and PEC force–elongation relation) of a total of four model [CC] relationships are realistic, the fitted active force–length relationship underestimates experimental data (Fig. 3) and suggests the presence of effects not accounted for in the model.

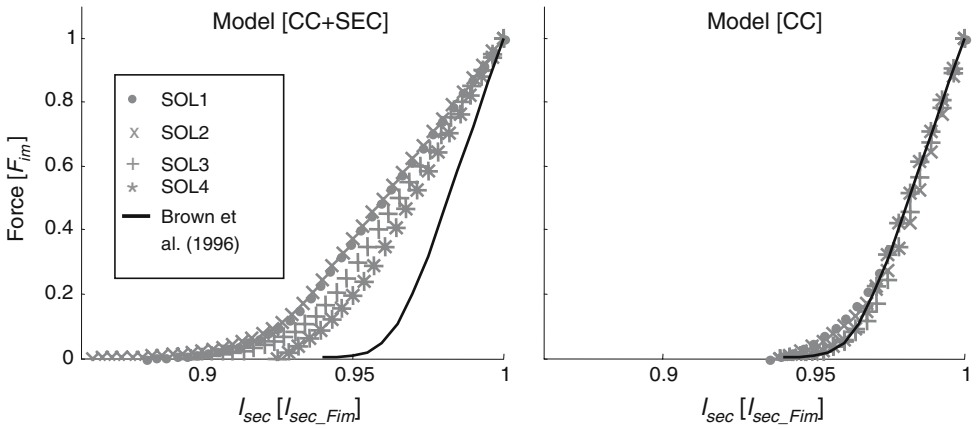

Fig. 6 Fitted force–strain relations based on model [CC+SEC] and model [CC] (*symbols*). SEC lengths were normalized relative to SEC length at F_{im} for comparison with the normalized SEC force–strain relation of cat soleus given by Brown et al. (1996) (*black line*). SEC length at F_{im} was estimated to be 65 mm (Rode et al. 2007), resulting in a SEC stiffness of 9.4 N/mm in the linear part for the literature relation

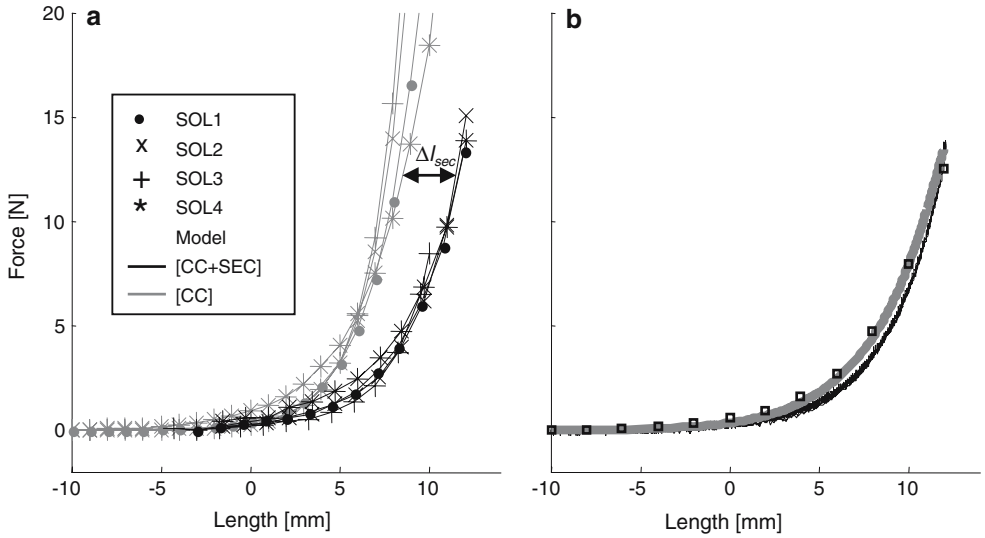

Fig. 7 Passive force–length relations. **a** PEC force–length relations equalling the passive muscle force–length relations for model [CC+SEC] (*black lines*) and PEC force–elongation relations shifted by model slack length $l_{\mathrm{mslack}} = -10$ mm for model [CC] (*grey lines*). The horizontal difference between the curves results from SEC elongation (Δl_{sec}) in model [CC]. **b** Passive force–length relations of SOL1 resulting from isometric experiments (*squares*) and passive ramp experiments (*black lines*) with different shortening velocities (5, 10, 20, 40, 70, 100 and 150 mm/s). The *grey line* shows the passive model [CC] force–length relation resulting from in series arrangement of SEC and PEC force–elongation relations using fitted model parameters (Table 2)

4.3 Underestimation of experimental isometric force–length relation by regression

The isometric force in muscle following shortening against resistance was found to be lower compared to the isometric force at the same length (e.g., Abbot and Aubert 1952). This effect is called force depression. Active force–length relationships resulting from regression to ramp experiments underestimated the experimental active force–length relationships (Fig. 3, model [CC]) determined from isometric experiments. Herzog et al. (2000) found force depression to be linearly related to the mechanical work performed by the muscle during shortening up to 10 mm (Fig. 8, black line). Plotting the determined force decrease as a function of the active work performed during the 5 mm/s ramps for each muscle resulted in a similar relation (Fig. 8) up to 20 mm shortening, suggesting that the underestimation of the active force–length relationship is mainly related to force depression. However, the slope of this linear relation was steeper, and for longer shortening distances the amount of force decrease was reduced (Figs. 8, 4, Model [CC]).

4.4 Relevance of passive forces in muscle modelling

There are numerous studies using Hill-type muscle models neglecting passive force for simulation of human movement (e.g., van Soest and Bobbert 1993; Geyer et al. 2003). This may be appropriate if all muscles work in a range with

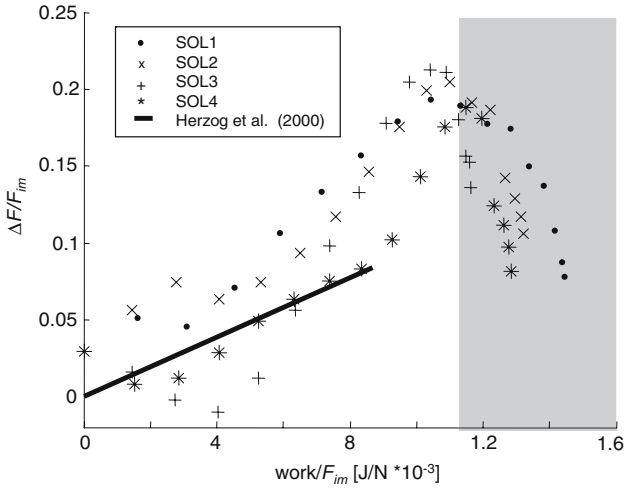

Fig. 8 Isometric force decrease as a function of normalized work (model [CC]). *Symbols* represent the force differences (ΔF) between experimental active force–length relationships (Fig. 3e–h, *filled circles*) and fitted active force–length relationships (Fig. 3e–h, *grey lines*). The work was calculated from the isokinetic part of the 5 mm/s ramp experiment. The *black line* shows the intermediate force depression in six cat soleus muscles measured in different experiments applying shortening distances up to 10 mm (Herzog et al. 2000). The data of Herzog et al. were normalized to a maximal isometric force of 23 N. The grey area illustrates shortening distances larger than 20 mm

negligible passive force. However, passive forces become increasingly important on the descending limb of the force–length relationship (e.g., Gareis et al. 1992).

A number of muscles were reported to work in this range, e.g., the human M. vastus lateralis during cycling (Muraoka et al. 2001) or shoulder muscles during arm abduction (Klein Breteler et al. 1999). A review of force–length operating ranges of vertebrae muscles is given by Burkholder and Lieber (2001), substantiating the necessity of modelling passive forces for certain muscles.

In fact, any stretching activities include passive muscle forces. During accidents like, e.g., automobile collisions maximal joint excursions and maximal muscle lengthening may occur. To predict injuries and to develop protective interventions, muscle-skeletal models including passive forces (model [CC+SEC]) were used to simulate whole body movement during crash tests (Hardin et al. 2004).

Additional relevance for muscle models including passive forces may arise from studies examining changing muscle properties of older people. Thelen (2003) showed that passive muscle stiffness increased and maximum isometric muscle force decreased with age.

Furthermore, passive forces do not scale with activation or velocity like the active forces and therefore may gain importance in submaximal conditions and fast movements. These considerations suggest that passive forces have to be accounted for appropriately.

Acknowledgments This work was supported by the German Science Foundation (DFG) grant Bl236/13-1.

References

Abbot BC, Aubert XM (1952) The force exerted by active striated muscle during and after change of length. J Physiol 117:77–86

Ahearn TS, Staff RT, Redpath TW, Semple SI (2005) The use of the Levenberg–Marquardt curve-fitting algorithm in pharmacokinetic modelling of DCE-MRI data. Phys Med Biol 50(9):85–92

Blickhan R, Wagner H, Seyfahrt A (2003) Brain or muscles? Recent Res Dev Biomech 1:215–245

Brown IE, Scott SH, Loeb GE (1996) Mechanics of feline soleus: II. Design and validation of a mathematical model. J Muscle Res Cell Motil 17:221–233

Brown IE, Cheng EJ, Loeb GE (1999) Measured and modeled properties of mammalian skeletal muscle. II. The effects of stimulus frequency on force–length and force–velocity relationships. J Muscle Res Cell Motil 20(7):627–643

Burkholder TJ, Lieber RL (2001) Sarcomere length operating range of vertebrate muscles during movement. J Exp Biol 204(9):1529–1536

Curtin NA, Gardner-Medwin AR, Woledge RC (1998) Predictions of the time course of force and power output by dogfish white muscle fibres during brief tetani. J Exp Biol 201:103–114

Epstein M, Wong M, Herzog W (2006) Should tendon and aponeurosis be considered in series? J Biomech 39(11):2020–2025

Ettema GJ, Meijer K (2000) Muscle contraction history: modified Hill versus an exponential decay model. Biol Cybern 83(6):491–500

Fung YC (1993) Biomechanics: mechanical properties of living tissues. Springer, New York

Gareis H, Solomonow M, Baratta R, Best R, D'Ambrosia R (1992) The isometric length-force models of nine different skeletal muscles. J Biomech 25(8):903–916

Geyer H, Seyfarth A, Blickhan R (2003) Positive force feedback in bouncing gaits? Proc Biol Sci 270:2173–2183

Hardin EC, Su A, Bogert AJ (2004) Foot and ankle forces during an automobile collision: the influence of muscles. J Biomech 37(5):637–644

van den Herzog W, Leonard TR (1997) Depression of cat soleus-forces following isokinetic shortening. J Biomech 30(9):865–872

Herzog W, Leonard TR (2000) The history dependence of force production in mammalian skeletal muscle following stretch-shortening and shortening stretch cycles. J Biomech 33(5):531–545

Herzog W, Kamal S, Clarke HD (1992) Myofilament lengths of cat skeletal muscle: theoretical considerations and functional implications. J Biomech 25(8):945–948

Herzog W, Leonard TR, Stano A (1995) A system for studying the mechanical properties of muscles and the sensorimotor control of muscle forces during unrestrained locomotion in the cat. J Biomech 28(2):211–218

Hill AV (1938) The heat of shortening and the dynamic constants of muscle. Proc R Soc Lond 126:136–195

Klein Breteler MD, Spoor CW, Van der Helm FC (1999) Measuring muscle and joint geometry parameters of a shoulder for modeling purposes. J Biomech 32(11):1191–1197

Marechal G, Plaghki L (1979) The deficit of the isometric tetanic tension redeveloped after a release of frog muscle at a constant velocity. J Gen Physiol 73(4):453–467

Muraoka T, Kawakami Y, Tachi M, Fukunaga T (2001) Muscle fiber and tendon length changes in the human vastus lateralis during slow pedaling. J Appl Physiol 91(5):2035–2040

Otten E (1987) A myocybernetic model of the jaw system of the rat. J Neurosci Methods 21:287–302

Proske U, Morgan DL (1984) Stiffness of cat soleus muscle and tendon during activation of part of muscle. J Neurophysiol 52:459–468

Rack PMH, Westbury DR (1969) The effects of length and stimulus rate on tension in the isometric cat soleus muscle. J Physiol 204(2):443–460

Rode C, Siebert T, Herzog W, Blickhan R (2007) The effects of parallel and series elastic components on estimated active cat soleus muscle force. Acta Physiol (submitted)

Scott SH, Brown IE, Loeb GE (1996) Mechanics of feline soleus: I. Effect of fascicle length and velocity on force output. J Muscle Res Cell Motil 17:207–219

Siebert T, Sust M, Thaller S, Tilp M, Wagner H (2007) An improved method to determine neuromuscular properties using force laws – From single muscle to applications in human movements. Hum Mov Sci 26:320–341

Thelen DG (2003) Adjustment of muscle mechanics model parameters to simulate dynamic contractions in older adults. J Biomech Eng 125(1):70–77

van Leeuwen JJ (1992) Muscle function in locomotion. In: Alexander RMcN (ed) Comparative and environmental Physiology. Mechanics of animal locomotion, vol 11. Springer, Berlin, pp 191–250

van Soest AJ, Bobbert MF (1993) The contribution of muscle properties in the control of explosive movements. Biol Cybern 69(3):195–204

van Soest AJ, Haenen WP, Rozendaal LA (2003) Stability of bipedal stance: the contribution of cocontraction and spindle feedback. Biol Cybern 88(4):293–301

Wagner H, Blickhan R (2003) Stabilizing function of antagonistic neuromusculoskeletal systems: an analytical investigation. Biol Cybern 199:163–179

Wagner H, Siebert T, Ellerby DJ, Marsh RL, Blickhan R (2005) ISOFIT—A model-based method to measure muscle-tendon properties simultaneously. J Biomech Model Mechanobiol 4:10–19

Wagner H, Thaller S, Dahse R, Sust M (2006) Biomechanical muscle properties and angiotensin-converting enzyme gene polymorphism: a model-based study. Eur J Appl Physiol 98(5):507–515

Winters JM, Woo SLY (1990) Multiple muscle system. Springer, New York